

## Supporting Information: Disposable Cartridge Platform for Rapid Detection of Viral Hemorrhagic Fever Viruses

Steven Scherr<sup>1</sup>, David Freedman<sup>2</sup>, Krystle N. Agans<sup>3,4</sup>, Alexandru Rosca<sup>2</sup>, Erik Carter<sup>5</sup>, Melody Kuroda<sup>6</sup>, Helen Fawcett<sup>1</sup>, Chad E. Mire<sup>3,4</sup>, Thomas W. Geisbert<sup>3,4</sup>, M. Selim Ünlü<sup>7,8,9</sup>, John Connor<sup>5,8</sup>

<sup>1</sup> Department of Mechanical Engineering, Boston University, Boston, MA 02215, <sup>2</sup> Nexgen Arrays, Boston, MA, 02215, <sup>3</sup> Galveston National Laboratory and <sup>4</sup> Department of Microbiology and Immunology, University of Texas Medical Branch, Galveston, TX, 77555, <sup>5</sup> Department of Microbiology, Boston University School of Medicine, Boston, MA, 02215, <sup>6</sup> BD, Research Triangle Park, NC, 27709, <sup>7</sup> Department of Electrical Engineering, Boston University, Boston, MA 02215, <sup>8</sup> Department of Biomedical Engineering, Boston University, Boston, MA 02215, <sup>9</sup> Physics Department, Boston University, Boston, MA 02215

### Flow Rate Optimization

Aside from the obvious advantages of a microfluidic flow cell, such as smaller sample volume, the miniaturized design offers benefits of increased surface area to volume ratio and improved mass transport<sup>1</sup>. Most micro-well plate based assays are diffusion limited and thus the reaction often takes hours to reach completion. Studies have shown that conducting this reaction in a flow cell can increase the binding rate by increasing the proximity of the capture molecule to the sensor and constantly replenishing any sample depletion<sup>2</sup>.

By intelligently designing the assay parameters, such as channel geometry and flow rate, the binding rate can be optimized. This has the potential to increase the sensitivity as well as reduce the time needed for incubation. Due to sample volume restrictions, flow rates ranging from 0.1-10  $\mu\text{L}/\text{min}$  were explored, which produce a Reynolds number well within the laminar flow regime. The low aspect ratio of our channel also allows us to safely assume the flow profile has a parabolic dependence on the height above the sensor as described by Poiseuille flow. During flow, particles move past the sensor more quickly than they can diffuse to the surface, as would be the case for moderately fast flow, and only particles very close to the sensor surface in what is called the depletion zone will be captured. By examining the flux of particles through this depletion zone, we can estimate how changing parameters such as flow rate, channel height, or channel width will impact the binding rate<sup>1</sup>. The expected relation is:

$$F \propto (Q/(H^2 W))^{1/3}$$

The width (W) is restricted by the number of spots in the microarray we want to fit in the channel and has been set to 2mm wide. The height (H) is limited by availability of commercial products, and thus 0.001 in (25.4 $\mu\text{m}$ ) is the thinnest we can reasonably make our channel. However if we can increase the flow rate (Q) we expect to see a modest increase in the flux of particles (F) and therefore binding rate. To achieve this, a syringe pump was used to deliver the sample to the incubation cartridge.

In order to determine the optimal flow rate, a sample was prepared of PBS with 1% BSA containing the model virus, rVSV-ZEBOV. This sample was driven through the cartridge with a syringe pump at flow rates of 0, 0.1, 1, and 10  $\mu\text{L}/\text{min}$ . Each flow rate was maintained for 15 minutes before changing to the next flow rate sequentially in a single experiment. The results of this experiment are seen in Figure 1A. Each color in Figure 1A corresponds to a different flow rate ranging from static (blue) ascending to 10  $\mu\text{L}/\text{min}$  (purple). This experiment was repeated with both ascending and descending flow conditions, which showed the same trend. To quantify and compare the effectiveness of each flow rate, a linear trend was fitted to each color line to give the number of viruses bound per spot per minute. This binding rate was reported in Figure 1B. Each color again corresponds to a different flow rate, with error bars representing the standard deviation of three different trials. This demonstrates a modest increase in binding rate with increased flow rate as predicted by the flux equation. The highest flow rate of 10  $\mu\text{L}/\text{min}$  (purple) is not significantly better than 1  $\mu\text{L}/\text{min}$  (green). The greater sample volume required to run an experiment at a higher flow rate is also detrimental. Therefore these results suggest that the optimal flowrate given realistic constraints is approximately 1  $\mu\text{L}/\text{min}$ , but that some variation is permitted without creating large experimental variability.

### Cartridge Design

A polymer laminate approach was taken to produce the cartridge due to its low cost and ability to produce high fidelity, low aspect ratio features. The polymer laminate approach can be scaled using a real-to-real process to reduce cost at high volume production. The final device incorporates 7 different layers as well as a luer reservoir not pictured in figure 2. Layer 1 acts as a base layer and is made of 0.060" acrylic. This layer is designed to give the cartridge structural rigidity for both the user and to support the additional layers. The square cut out in layer 1 is to accommodate placement of the sensor

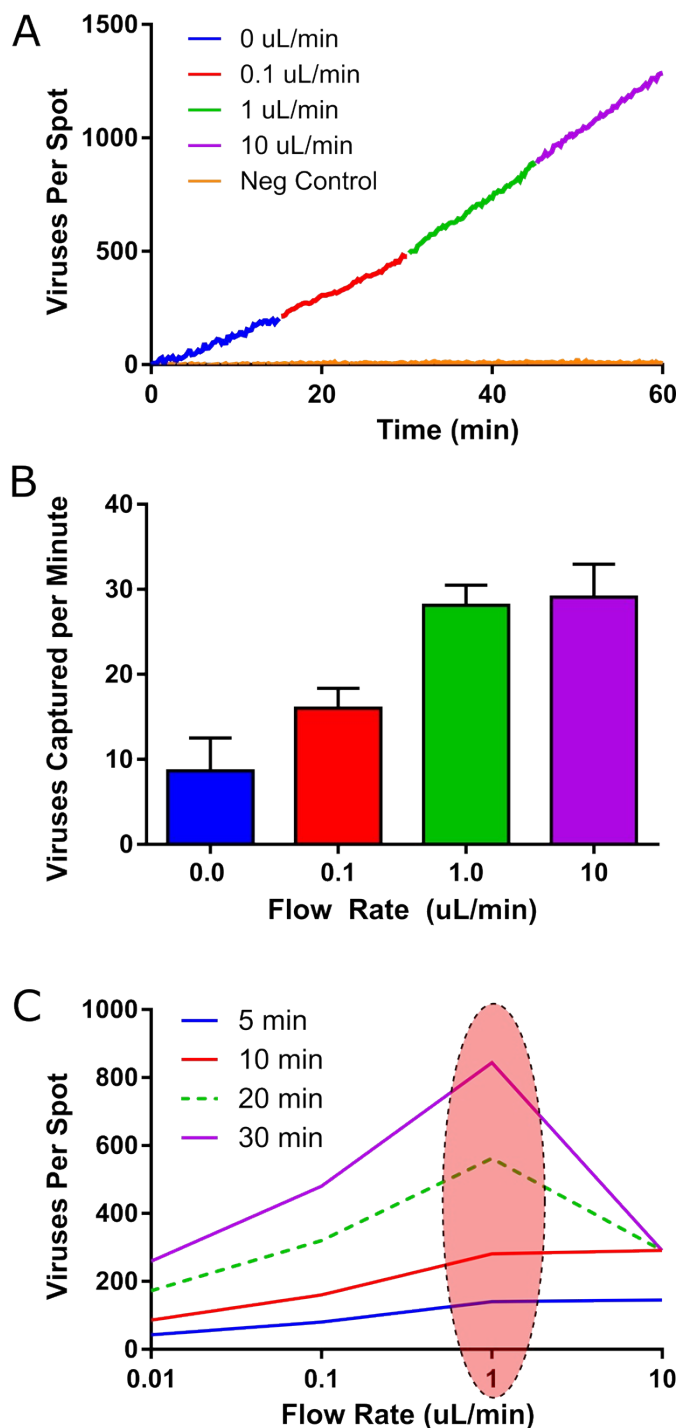


Figure 1. Flow rate optimization. A) shows the number of viruses captured versus time for an ascending flow rate experiment. The negative control shows no binding and remains effectively at zero. B) shows the first order quantification of the virus capture rate of 3 different trials of virus binding experiments. C) shows the theoretical virus capture for each flow rate with a 100  $\mu\text{L}$  sample volume and different total experimental time.



Figure 2. Cartridge design shows the 7 layers used to produce the device as well as the completed device at the top. The materials and thicknesses are labelled next to each layer.

in the cartridge. Layer 2 is a 0.001" silicone pressure sensitive adhesive (PSA) layer. This layer is used to bond the sensor into the cartridge. There are two cuts in layer 2; the solid line indicates a through cut and defines the dimensions of the flow channel on top of the sensor. The dotted line is a partial cut through the release liner that facilitates removal of the liner when installing the sensor. Layer 3 is a 0.005" polycarbonate layer. Layer 3 acts a viewing window for imaging the sensor through. This layer has through holes that allow the sample to flow down through layer 3 into the channel in layer 2 below. Layer 4 is a 0.003" silicone PSA layer. This layer defines the channels that allow flow from the luer sample reservoir (not shown) to the sensor as well as a cut out for the absorbent pad. The square cut out in the center of layer 4 is to allow unobstructed imaging of the polycarbonate window. Layer 5 is the absorbent pad (CF1 - General Electric). The pad absorbent shape is discussed further in the main text. Layer 6 is a 0.002" PET layer that seals the channels below. This layer has an inlet hole under the sample reservoir and vent hole above the absorbent pad to allow air the exit as fluid fills the pad. There is also a square cut out in this layer to allow imaging of the sensor. Layer 7 is a 0.060" acrylic layer with silicone PSA attached. This layer acts as structural support for the luer sample reservoir and has a circular hole cut to hold the reservoir. The reservoir is placed and glued into the hole in layer 7. The completed device is shown at the top of figure 2 to show how the channels in different layers line up to allow continuous flow through the cartridge. These devices were prototyped and fabricated with help from the State of Utah Center of Excellence for Biomedical Microfluidics and Aline Inc.

- 1 T. M. Squires, R. J. Messinger and S. R. Manalis, *Nature biotechnology*, 2008, **26**, 417–26.
- 2 H. Parsa, C. D. Chin, P. Mongkolwisetwara, B. W. Lee, J. J. Wang and S. K. Sia, *Lab on a chip*, 2008, **8**, 2062–70.